

Single-Step Fabrication of Transparent Superhydrophobic Porous Polymer Films

Hiroshi Yabu^{*,†,‡} and Masatsugu Shimomura^{*,†,‡,§}

Nanotechnology Research Center, Research Institute for Electronic Science, Hokkaido University, N21W10, Sapporo 001-0021, Japan, Frontier Research System, Institute of Physical and Chemical Research (RIKEN Institute), 1-12, Hirosawa, Wako, Saitama 351-0198, Japan, and Core Research for Evolutional Science and Technology (CREST), Japan Science and Technology Agency (JST), 4-1-8, Honmachi, Kawaguchi, Saitama 332-0012, Japan

Received June 14, 2005

Revised Manuscript Received September 11, 2005

Water repellency is very useful for applications such as dust-free coatings, coverings to prevent snow sticking, and others.¹ Water repellency is dominated by the topology and chemistry of surfaces. For a flat surface, theoretical calculation shows that densely packed CF₃ groups would give the highest water contact angle possible, 120°. In nature, however, superhydrophobic surfaces have been found with water contact angles higher than 120°. Lotus leaf, for example, secretes waxy compounds on its rough surface, which is covered in many small bumps.³ The water repellency of plant leaves is due to this surface roughness enhancing the hydrophobicity. The water contact angle of the rough surface, θ_w , is described by Wenzel's equation,⁴

$$\cos \theta_w = r \cos \theta$$

where r is the roughness factor and θ is the contact angle for a flat surface. The roughness factor, r , is the ratio of the actual surface area to the apparent surface area of the substrate. The superficial contact angle of a surface composed of two components (e.g., air and polymer) is also given by a formula reported by Cassie⁵ based on the fraction of each component's surface area. According to Cassie's law,

$$\cos \theta_c = \phi_1 \cos \theta_1 + \phi_2 \cos \theta_2$$

where θ_c is the superficial contact angle; θ_1 and θ_2 are contact angles of flat films of components 1 and 2, respectively; and ϕ_1 and ϕ_2 are surface area fractions of polymer and air, respectively. Rough or microstructured surfaces are required to form the surface with contact angles of water higher than 150°. ^{6–12}

For superhydrophobic surface applications such as optical coatings for window glass or painted surfaces, optical transparency is also important. Microstructured surfaces are, however, not transparent due to Mie scattering¹³ from their rough surfaces. In the case of the surface structures larger than the visible light wavelength, the Mie scattering has occurred. In this case, the wide range of irradiated light is scattered by the structured surface depending on the size of surface structures, incident angles of light irradiation, and differences of refractive indices between the air and materials. As the result, the structured surface looks opaque. To achieve optical transparency, the size of the underlying structure should be smaller than the wavelength of visible light (at least <400 nm). Therefore, a transparent and superhydrophobic surface requires a highly rough surface on the sub-wavelength scale. Some papers reported the preparation of a transparent superhydrophobic surface by preparing a small roughness onto inorganic oxides.¹⁴

Honeycomb-like microporous polymer films with 500 nm to 50 μ m pores (diameter) have been prepared by casting polymer solutions under humid conditions.^{15–18} Using this method, we have prepared honeycomb-patterned polymer films as potential functional materials including engineering (e.g., polystyrene) and super-engineering plastics (e.g., polyimide),¹⁹ biodegradable polymers,²⁰ and titanium oxide.²¹ Recently, we have reported that the honeycomb-patterned

* To whom correspondence should be addressed. Tel. & fax: +81-11-706-9369. E-mail: yabu@poly.es.hokudai.ac.jp.

[†] Hokkaido University.

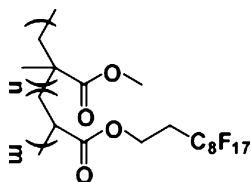
[‡] Institute of Physical and Chemical Research (RIKEN Institute).

[§] Japan Science and Technology Agency (JST).

- (1) Ball, P. *Nature* **1999**, *400*, 507.
- (2) Hozumi, A.; Takai, O. *Thin Solid Films* **1997**, *303*, 222–225.
- (3) (a) Barthlott, W.; Neinhuis, C. *Planta* **1997**, *202*, 1, (b) Otten, A.; Herminghaus, S. *Langmuir* **2004**, *20* (6), 2405.
- (4) Wenzel, R. N. *Ind. Eng. Chem.* **1949**, *28*, 988.
- (5) Cassie, A. B. D. *Discuss Faraday Soc.* **1948**, *3*, 11.
- (6) Tada, H.; Nagayama, H. *Langmuir* **1995**, *11* (1), 136.
- (7) Öner, D.; McCarthy, T. J. *Langmuir* **2000**, *16* (20), 7777.

- (8) (a) Onda, T.; Shibuichi, S.; Satoh, N.; Tsujii, K. *Langmuir* **1996**, *12*, 2125–2127. (b) Tsujii, K.; Yamamoto, T.; Onda, T.; Shibuichi, S. *Angew. Chem., Int. Ed. Engl.* **1997**, *36*, 1011–1012. (c) Shibuichi, S.; Yamamoto, T.; Onda, T.; Tsujii, K. *J. Colloid Interface Sci.* **1998**, *208*, 287–294.
- (9) (a) Miwa, M.; Nakajima, A.; Fujishima, A.; Hashimoto, K.; Watanabe, T. *Langmuir* **2000**, *16*, 5754–5760. (b) Nakajima, A.; Hashimoto, K.; Watanabe, T. *Monatsh. Chem.* **2001**, *132*, 31–41.
- (10) Wang, R.; Hashimoto, K.; Fujishima, A.; Chikuni, M.; Kojima, E.; Kitamura, A.; Shimohigoshi, M.; Watanabe, T. *Nature* **1997**, *388*, 431–432.
- (11) Bico, J.; Marzolin, C.; Quere, D. *Europhys. Lett.* **1999**, *47*, 220–226.
- (12) (a) Feng, L.; Li, S.-H.; Li, H.-J.; Zhai, J.; Song, Y.-L.; Jiang, L.; Zhu, D.-B. *Angew. Chem., Int. Ed.* **2002**, *41*, 1221. (b) Feng, L.; Li, S.-H.; Li, Y.-S.; Li, H.-J.; Zhang, L.-J.; Zhai, J.; Song, Y.-L.; Liu, B.-Q.; Jiang, L.; Zhu, D.-B. *Adv. Mater.* **2002**, *14*, 1857–1860. (c) Feng, L.; et al. *Angew. Chem., Int. Ed.* **2003**, *42*, 800–802. (d) Feng, L.; Song, Y.-L.; Zhai, J.; Liu, B.-Q.; Xu, J.; Jiang, L.; Zhu, D.-B. *Angew. Chem., Int. Ed.* **2003**, *42*, 4217–4220.
- (13) Mie, G. *Ann. Phys.* **1908**, *25*, 377.
- (14) (a) Nakajima, A.; Fujishima, A.; Hashimoto, K.; Watanabe, T. *Adv. Mater.* **1999**, *11*, 1365–1368. (b) Nakajima, A.; Hashimoto, K.; Watanabe, T.; Takai, K.; Yamauchi, A.; Fujishima, A. *Langmuir* **2000**, *16* (17), 7044.
- (15) (a) Widawski, G.; Rawiso, M.; François, B. *Nature* **1994**, *369*, 387–389. (b) François, B.; Pitois, O.; François, J. *Adv. Mater.* **1995**, *7*, 1041.
- (16) Govor, L.; Bashmakov, I.; Kiebooms, R.; Dyakonov, V.; Parisi, J. *Adv. Mater.* **2001**, *13*, 588. Stenzel, M. *Aust. J. Chem.* **2002**, *55*, 239–243.
- (17) Maruyama, N.; Koito, T.; Nishida, J.; Sawadaishi, T.; Cieren, X.; Ijiro, K.; Karthaus, O.; Shimomura, M. *Thin Solid Films* **1998**, *327*–329, 854.
- (18) Karthaus, O.; Maruyama, N.; Cieren, X.; Shimomura, M.; Hasegawa, H.; Hashimoto, T.; *Langmuir* **2000**, *16*, 6071–6076.
- (19) (a) Yabu, H.; Tanaka, M.; Ijiro, K.; Shimomura, M. *Langmuir* **2003**, *19*, 6297–6300. (b) Yabu, H.; Shimomura, M. *Langmuir* **2005**, *21* (5), 1709.
- (20) Nishikawa, T.; Ookura, R.; Nishida, J.; Arai, K.; Hayashi, J.; Kurono, N.; Sawadaishi, T.; Hara, M.; Shimomura, M. *Langmuir* **2002**, *18*, 5734–5740.

Chart 1



films of fluorinated polymers show superhydrophobicity.²² However, the films formed were not transparent because the pore size was larger than 1 μm . In the present report we have succeeded in reducing the pore size of honeycomb-patterned fluorinated polymer films to below sub-wavelength. Scanning electron microscopy reveals that the sub-wavelength pores (the smallest size ~ 100 nm) were generated by rapid solvent evaporation. The effect of pore size on water repellency and transparency of the prepared honeycomb-patterned films is discussed.

Copolymer 1,²³ having equimolar amounts of fluorinated acrylate and methyl methacrylate monomers, was kindly provided by Asahi Glass Co., Japan (Chart 1, molecular weight = 39 000, $T_g = 50.1$ °C). For the experiments, the copolymer was dissolved in a fluorinated solvent (AK-225, a mixture of $\text{CF}_3\text{CF}_2\text{CHCl}_2/\text{CClF}_2\text{CHClF}$, Asahi Glass Co., Japan) at a concentration of 1.5 mg/mL.

A glass substrate (76 mm \times 26 mm) was cleaned by UV–ozone treatment for 30 min (Ai ozone cleaner, Iwasaki Denki, Japan) and ethanol. Immersion in a 2 wt % AK-225 solution of 1*H*,1*H*,2*H*,2*H*-perfluorooctylchlorosilane for 30 min gave a fluorinated surface. To complete the surface modification, the glass substrate was baked at 120 °C for 2 h in an electric oven.

The fluorinated glass substrate was fixed to a moving substrate holder,²¹ which was smoothly controlled by a computer-driven system (Figure 1). A metal blade was fixed perpendicular to the substrate, and the gap between the blade edge and the substrate was adjusted to about 100 μm . Fifty microliters of the fluorinated copolymer solution was cast on the substrate, and the substrate was moved in a straight line at 2 mm/s. The fluorinated copolymer solution was supplied to the gap between the blade and substrate. Then, humid air (relative humidity $\sim 60\%$ at room temperature) was applied to the solution surface with a flow velocity of 10 L/min. The formation of the honeycomb-patterned film was observed by an optical microscope (BH2, Olympus, Japan) and video recording system (DSR-30, Sony, Japan).

After evaporation of the solvent, the surface structure of the film was observed by a field-emission scanning electron microscope (FE-SEM, S-5200, Hitachi, Japan). The water contact angle on the honeycomb-patterned film was measured using a contact angle analyzer (G-1, ERMA, Japan). Ten microliters of membrane-filtered water was dropped onto the honeycomb-patterned films. The transmittance of the honeycomb-patterned films was measured using UV–vis

spectroscopy (Lambda S900, Perkin-Elmer, Germany). The surface area fraction of pore and polymer was calculated from the SEM images of prepared films by using an imaging soft, NIH image (National Institute of Health, U.S.A.).

The formation of microporous structure essentially consists of four steps: (1) condensation of water droplets at the solution surface, (2) growth of the water droplets, (3) packing of the water droplets by capillary forces, and (4) complete evaporation of the solvent and subsequent evaporation of the water droplets.¹⁷ Because the pores are formed based on the condensed water droplets as templates, size control of the condensed water droplets is important for regulation of the pore size. To produce a smaller pore size, the condensed water droplets should be small. We have previously reported that the pore size of honeycomb-patterned films can be controlled by the solvent evaporation time under a continuous supply of humid air. A larger application of casting solution gives a larger pore size for the honeycomb-patterned film. Consequently, immediate evaporation of the solvent is required to produce small pores.

To shorten the evaporation time, we reduce the thickness of the casting solution applied. In fact, the solvent evaporates immediately when the casting solution is spread as a homogeneous thin liquid film. For this purpose we have developed a simple device for supply of the polymer solution to the solid substrate as a thin liquid film (Figure 1). The solid substrate is fixed to a substrate holder that is moved horizontally. For application of the casting solution, a metal blade is fixed perpendicular to the substrate and the distance between the blade edge and the substrate surface is adjusted to less than 100 μm . Fifty microliters of polymer solution is cast on one side of the metal blade, and then the substrate is moved directly to the left side in Figure 1. As a result, the polymer solution is supplied as a thin liquid film from the narrow gap between the metal blade and the substrate.

The wettability of the substrate surface is important for the stability of the thin liquid film. Because the polymer and solvent are fluorinated in this experiment, the solution does not spread on a hydrophilic glass substrate, as a result of its low surface tension. Therefore, we modified the glass substrate using a fluorinated silane coupling agent. After modification, the contact angle of the fluorinated solvent on the substrate decreased to less than 10° and the solution spread homogeneously. By moving the substrate, the thin liquid film was applied while under a flow of humid air. The solvent immediately evaporated within one video frame (about 30 ms) as observed by the microscope.

Figure 2 shows FE-SEM images of the surface of the prepared film. On the front edge of the film, a random distribution of pores of varying size was observed. The pore size ranged from about 20 to 200 nm. The smallest pore size observed is comparable to the smallest theoretical size of a condensed water droplet at room temperature, 10 nm.²⁴ In contrast, at around 100 μm from the film edge, there is a regular arrangement of 100 nm pores. The pore size gradually increases to 300 nm with increasing distance from the film

(21) (a) Karthaus, O.; Cieren, X.; Maruyama, N.; Shimomura, M. *Mater. Sci. Eng. C* **1999**, *10*, 103. (b) Yabu, H.; Shimomura, M. *Int. J. Nanosci.* **2002**, *1* (5–6), 673.

(22) Shimomura, M.; Yabu, H.; Yamamoto, H.; Kaida, Y. Japanese Patent JP2005-023122, 2005.

(23) Yabu, H.; Shimomura, M. *Adv. Funct. Mater.* **2005**, *15* (4), 575.

(24) Kittel, C.; Kroemer, H. *Thermal Physics*; W. H. Freeman and Company: New York, 1980.

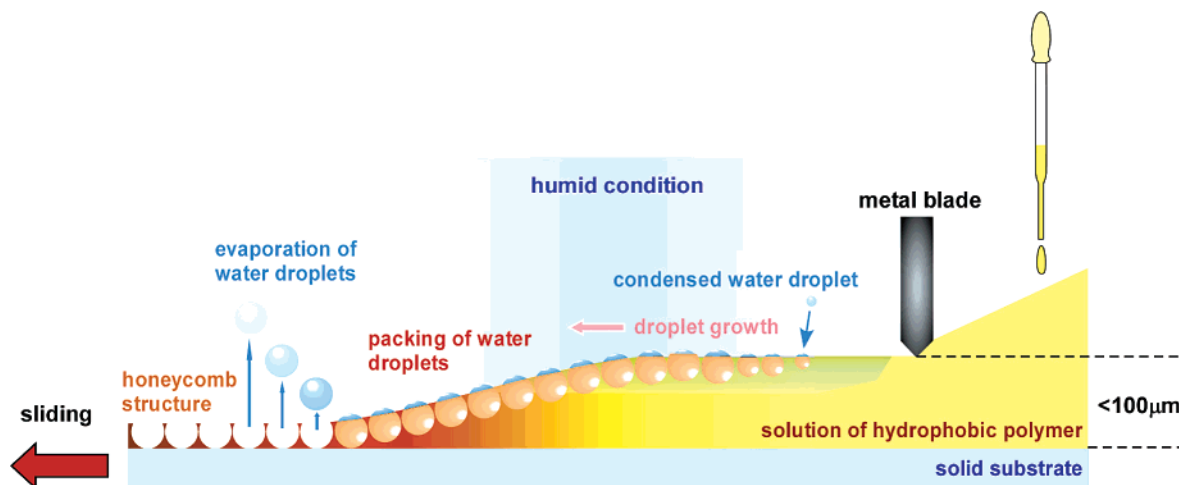


Figure 1. Schematic illustration of honeycomb-patterned film preparation.

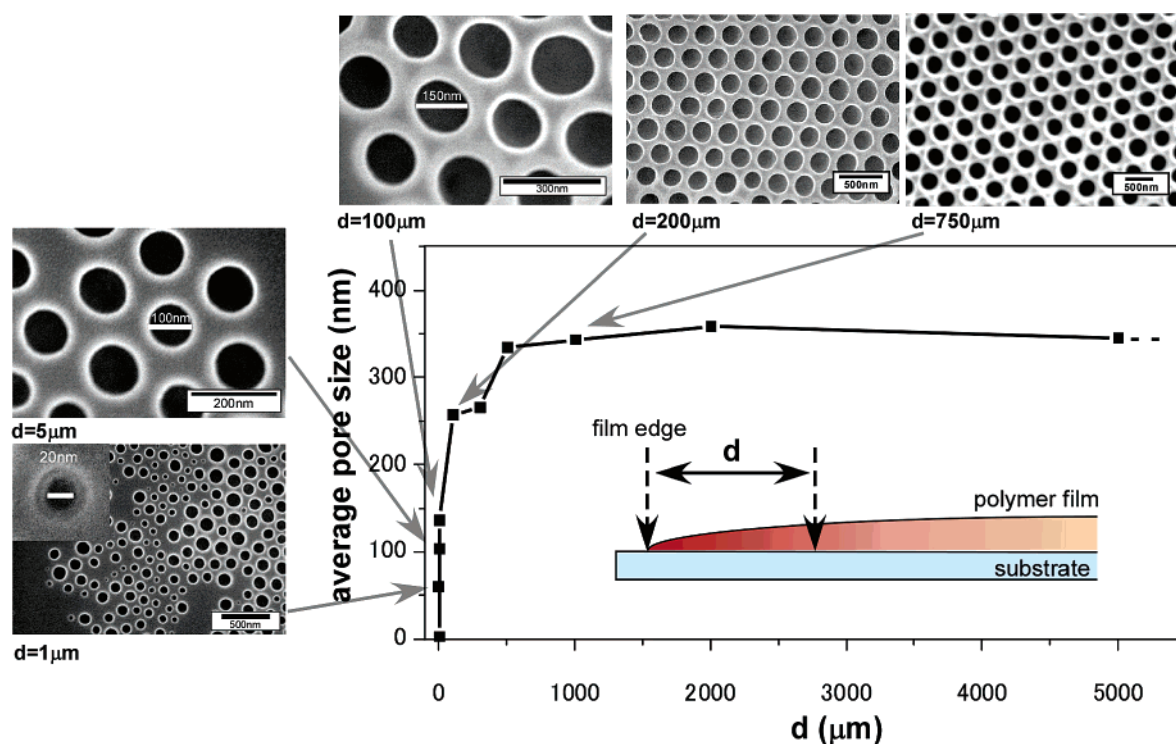


Figure 2. Plot of the average pore sizes and the distance from the film edge (d). FE-SEM images of the film surface taken on the different distances from the edge.

edge. Thus, under the described preparation conditions (humidity, temperature, moving speed), the pore size over the major part of the film was 300 nm.

Figure 2 indicates that the water droplet grows during their arrangement toward well-hexagonal packing. Thus, there is a tradeoff between reduction of the pore size and regular packing of the pores. In our case, the fast solvent evaporation rate applied to reduce the water droplet size seems to be balanced with a suitable time duration for regular arrangement of the condensed water droplets. The pore size of the honeycomb structure can be easily controlled up to 5 μm by changing the thickness of the liquid film from 100 μm to 1 mm.

We have previously reported that the water contact angle increases with decreasing pore size of the honeycomb-patterned fluorinated polymer.²⁵ The water contact angle on

honeycomb-patterned films with 300 nm pores was measured to be 160° (Figure 3a). The sub-wavelength structure enhances the hydrophobicity of rough surfaces. This value is higher than that of a 2- μm -pore honeycomb-patterned film (145°). This value is also higher than the theoretical value. The theoretical contact angle on the honeycomb-patterned film of 300-nm-sized pores was calculated by using Cassie's law. From the calculation of the surface area fraction of the polymer part by using imaging software, the fraction of the polymer part was 0.20–0.26. By using Cassie's equation, the theoretical water contact angle on the honeycomb-patterned film with 300 nm pores was up to about 153° (see Supporting Information). The high contact angle measured on the honeycomb-patterned film is due to the surface

(25) Yabu, H.; Takebayashi, M.; Tanaka, M.; Shimomura, M. *Langmuir* 2005, 21 (9), 3235.

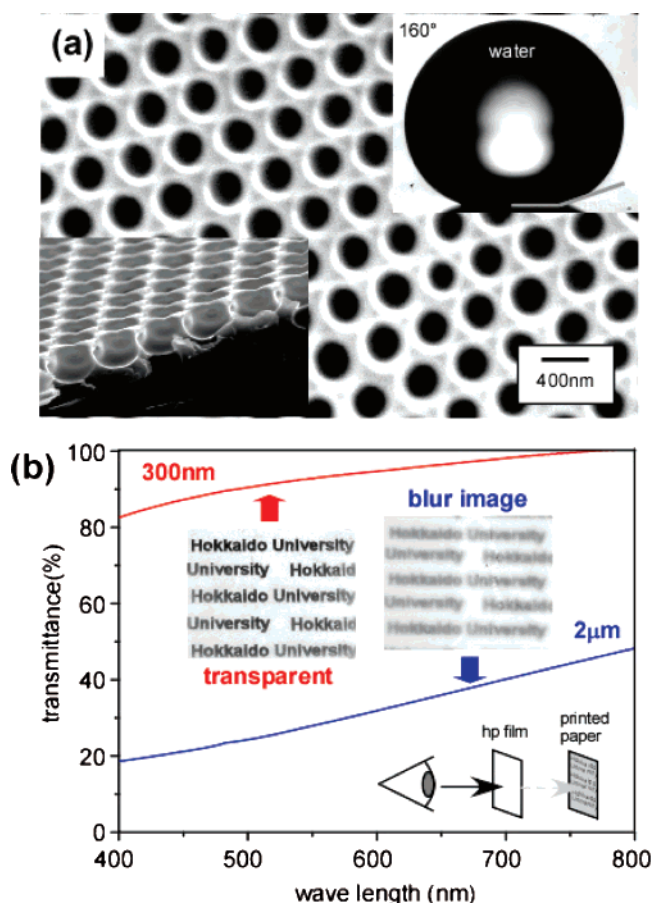


Figure 3. (a) Scanning electron micrograph of the 300-nm-sized honeycomb-patterned film (top image and cross section) and the water contact angle on this film. (b) Transmittance of the 2- μ m- and the 300-nm-sized honeycomb-patterned films and photograph of the film with printed papers underneath.

roughness of the rim of honeycomb pores (see the cross section of the film in the inset of Figure 3a). The vertex of hexagons is slightly higher than the other part of the rim. Thus, the real contact area is smaller than the calculated value from the top image.

Transmittances of the micrometer (2 μ m) and sub-wave-length (300 nm) honeycomb-patterned films were measured by UV–vis spectroscopy. Figure 3b clearly indicates that the transmittance of the 2- μ m-pore film is lower than 50% whereas that of the submicrometer-sized honeycomb-patterned film is higher than 80%. The 2- μ m-pore film is opaque, blurring the letters beneath the film (inset photograph in Figure 3b). On the other hand, the 300-nm-pore film is transparent enough to read the letters clearly through the film. It is also noted that the depths of the pores are also smaller than the visible wavelength (see cross-section image in Figure 3a). Thus, the film with 300 nm pores does not scatter light regardless of the incident light angles.

A simple method of preparing sub-wavelength-pore honeycomb-patterned films is demonstrated by casting of the polymer solution under humid conditions. By utilizing a specialized coating instrument we have developed, the thickness of the liquid film was reduced to less than 100 μ m. The sub-wavelength honeycomb-patterned films obtained are optically transparent and exhibit superhydrophobicity. The smallest pore size was 20 nm. Our method does not require expensive techniques such as chemical vapor deposition, etching, or UV exposure. Further, the films can be formed from a large variety of materials and on a wide variety of substrates. Such sub-wavelength honeycomb-patterned films have application as transparent and superhydrophobic polymer films.

Acknowledgment. We thank Dr. H. Yamamoto and Dr. Y. Kaida for providing the fluorinated polymers. This work was partly supported by Grant-in-aid for scientific research, MEXT, Japan.

Supporting Information Available: Calculation of the theoretical contact angle by Cassie's law. This material is available free of charge via the Internet at <http://pubs.acs.org>.

CM051281I